Polarimetric characterization of a monochromator to measure the spectral response of a pixelated polarization imager

Venkatesulu, Erica, Syed, Musaddeque, Shaw, Joseph

Erica Venkatesulu, Musaddeque A. Syed, Joseph A. Shaw, "Polarimetric characterization of a monochromator to measure the spectral response of a pixelated polarization imager," Proc. SPIE 11833, Polarization Science and Remote Sensing X, 118330G (1 August 2021); doi: 10.1117/12.2594011

SPIE.

Event: SPIE Optical Engineering + Applications, 2021, San Diego, California, United States

Polarimetric characterization of a monochromator to measure the spectral response of a pixelated polarization imager

Erica Venkatesulu[a], Musaddeque A Syed[a], and Joseph A Shaw[a]

[a]Electrical and Computer Engineering Department, Montana State University, P.O. Box 173780, Bozeman, USA

ABSTRACT

Monochromators are frequently used in spectral calibrations of optical systems due to their ability to sweep a narrowband output across a wide range of wavelengths. However, monochromators tend to output light with a degree of linear polarization that can vary significantly as a function of wavelength. To use a monochromator to calibrate a polarization-sensitive imager, the monochromator output is often passed into an integrating sphere to convert the linearly polarized light into randomly polarized light. In this paper, we demonstrate the ability to obtain a spectral calibration of a division-of-focal-plane (DoFP) imager by assuming subpixels of a polarization super pixel have equal spectral responses. We also characterize the polarization of the output of a monochromator as a function of wavelength using both a DoFP imager and a wire-grid polarizer mounted on a precision rotation stage with an optical power meter.

Keywords: monochromator, spectral response, polarization imaging

1. INTRODUCTION

Grating monochromators are used frequently for measuring the relative spectral response (RSR) function of an optical instrument.[1–5] Alternate methods include Fourier transform spectrometers (FTS),[6] tunable lasers,[7,8] tunable LEDs,[9] multiple spectral filters with broadband sources,[10] and stochastic optimization algorithms operating on colored sample and diffraction images.[11] However, the light output from Fourier transform spectrometers or monochromators can be significantly polarized, which complicates measuring the RSR of polarization-sensitive sensor systems. It is also important to note that polarization sensitivity in optical systems can be intentional[12,13] or unintentional.[14–18] If the source light is input to the system being calibrated through an integrating sphere, the polarization state of the monochromator output may be negligible, but this approach often results in light-starved measurements and is therefore not always possible or desirable. This paper discusses the use of a grating monochromator to measure the RSR function of a polarization-sensitive imager. In this case, the imager used a division-of-focal-plane (DOFP)[12,19] detector array so we were able to combine measurements from differently polarized adjacent pixels to determine the linear Stokes parameters and Degree of Linear Polarization (DoLP) for the monochromator output. This also allowed calculation of an S_0 Stokes parameter at each wavelength, thereby enabling us to determine the RSR for the polarization imager.

2. MONOCHROMATOR AND DOFP IMAGER SYSTEMS

A monochromator operates as a grating spectrometer in reverse, dispersing light from a broadband source into a spectrum using a diffraction grating on a rotation stage. The layout of the monochromator used in this study, the Acton Research Corporation SP-150, is shown in Fig. 1. Broadband light from a halogen light source enters the system through the entrance slit on the right and is reflected from two mirrors. It is then reflected from a diffraction grating, which disperses the light into a spectrum. The dispersed light is reflected from a final mirror, and the output slit selects a portion of the spectrum that exits the system. The diffraction grating can be rotated to control the portion of the spectrum exiting the system, and the output slit width can be adjusted to control the bandwidth of the output. The monochromator in the measurements reported here used a blazed grating with 300 grooves/mm, and the output slit width was 3 mm.

Further author information:
Joseph A. Shaw: E-mail: joseph.shaw@montana.edu, Telephone: 406-994-7261

Polarization Science and Remote Sensing X, edited by Meredith K. Kupinski, Joseph A. Shaw, Frans Snik, Proceedings of SPIE Vol. 11833, 118330G · © 2021 SPIE
CCC code: 0277-786X/21/$21 · doi: 10.1117/12.2594011

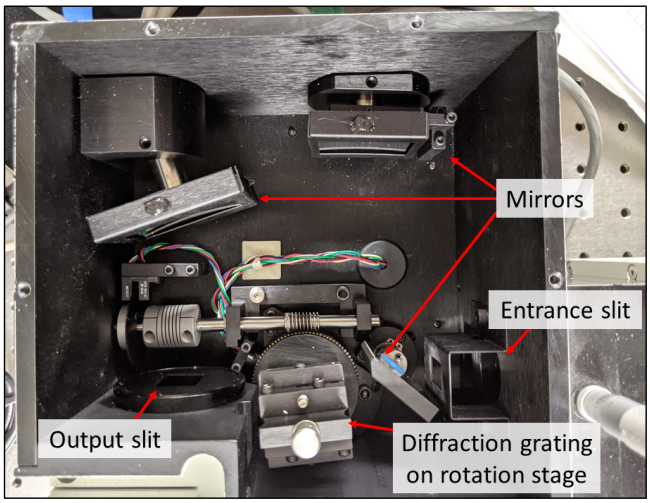

Figure 1. Top-down view of the inside of the Acton Research Corporation SP-150 monochromator. Light entering through the entrance slit is reflected from two mirrors, a diffraction grating, and another mirror before exiting through the output slit.

For polarization mechanisms, we start by recognizing that lamp filaments can emit partially polarized light, especially when viewed at oblique angles.[20–23] Beyond this, there are two primary mechanisms by which the light from the halogen lamp can become further polarized. First, when light is incident a on mirror at an oblique incidence angle, the two orthogonal polarization components (parallel and perpendicular to the plane of incidence) are reflected by different amounts, according to the Fresnel coefficients. This results in partial polarization of the reflected light. Second, the polarization state of light diffracted by a grating varies with wavelength and incidence angle. This causes the polarization state of the output light to vary as the wavelength is adjusted by the changing angle of incidence on the diffraction grating. This poses no problem for sensor systems with negligible polarization sensitivity, but can result in large errors for systems with significant polarization sensitivity.

Questions about the polarization state of our monochromator output arose when we began investigating the spectral response of pixelated DoFP imagers[12] that use the recently released Sony polarization-sensitive sensor.[19] These imagers measure the polarization of incident light using an array of wire-grid polarizers placed on top of the detector, oriented such that the four subpixels in a 2x2 group of pixels (referred to as a super pixel) measure four different linear polarization states. Relative to horizontal, the four linear polarization states passed by the wire-grid polarizers are 90 degrees for the top left subpixel, 45 degrees for the top right subpixel, 0 degrees for the bottom right subpixel, and 135 degrees for the bottom left subpixel of each super pixel. Thus, once a radiometric calibration is performed on the imager, a super pixel can measure the incident irradiances I_{0°, I_{45°, I_{90°, and I_{135° in its instantaneous field of view. With these four irradiances, the linear Stokes vector can be determined as follows:

$$S_0 = I_{0^\circ} + I_{90^\circ} \tag{1}$$

$$S_1 = I_{0^\circ} - I_{90^\circ} \tag{2}$$

$$S_2 = I_{45^\circ} - I_{135^\circ} \tag{3}$$

Using the linear Stokes parameters, the degree of linear polarization (DoLP) and angle of polarization (AoP) of the light can be determined. The DoLP is given by

$$DoLP = \frac{\sqrt{S_1^2 + S_2^2}}{S_0} \tag{4}$$

and the AoP is given by

$$AoP = \frac{1}{2} \arctan \frac{S_2}{S_1} \,. \tag{5}$$

3. MONOCHROMATOR OUTPUT POLARIZATION MEASUREMENTS

The state of polarization of the monochromator output light was measured using two DoFP cameras (FLIR BFS-U3-51S5P and Lucid Vision Labs TRI050S-PC) and confirmed using an optical power meter (Newport 1830-C) and a custom-built polarizer (Meadowlark Optics Versalight - aluminum wire grid on UV grade fused silica substrate) on a precision rotation stage (Newport RV160CC). First, the camera was aligned so that the monochromator output was incident directly on the camera sensor. The data from corresponding subpixels were combined to form I_{0°, I_{45°, I_{90°, and I_{135° images. A region of interest was identified, which contained the area of the detector on which the output of the monochromator was incident. The pixel values in the region of interest were averaged to form an average I_{0°, I_{45°, I_{90°, and I_{135° value for each wavelength output by the monochromator, and these four averages were used to calculate an average S_0, S_1, and S_2 over a region of interest. Finally, the average S_0, S_1, and S_2 were used to find an average DoLP and AoP using Eqs. 4 and 5. This process was repeated for both the FLIR and Lucid cameras.

In order to verify the measurements made with the FLIR and Lucid cameras, independent measurements of I_{0°, I_{45°, I_{90°, and I_{135° were made using an optical power meter and a wire-grid polarizer mounted on a precision rotation stage. These measurements were made at the wavelengths found to correspond to DoLP maxima and minima with the DoLP camera. Figures 2 and 3 show the DoLP and AoP measured by the cameras and by the combination of optical power meter and polarizer. We found that the output of the monochromator swung from highly polarized, with DoLP maxima greater than 0.7, to nearly randomly polarized, with DoLP minima less than 0.1. The output had AoP = 90 degrees (relative to horizontal) for most of the spectral range of the DoFP cameras, but it had AoP = 0 degrees from 508 to 564 nm. The discrepancies between the measurements made by the camera and by the optical power meter and polarizer setup are attributed primarily to spatial variations in the output of the monochromator as a function of wavelength. These variations resulted in partial detector illumination at some wavelengths and made it difficult to choose a region of interest that was applicable at all wavelengths.

4. RELATIVE SPECTRAL RESPONSE MEASUREMENTS

Spectral characterizations are performed to understand the relative spectral response (RSR) of a detector. Typically, a narrowband source of known output power is incident on the detector and swept across the spectral range of the detector to measure the RSR. If the source is not randomly polarized and the detector system has non-negligible polarization sensitivity (whether intentional or incidental), the measured RSR will contain polarization artifacts, causing the measured RSR to deviate from the true RSR. For the DoFP camera detectors used in this study, the individual subpixels cannot be measured with a monochromator because of its strongly

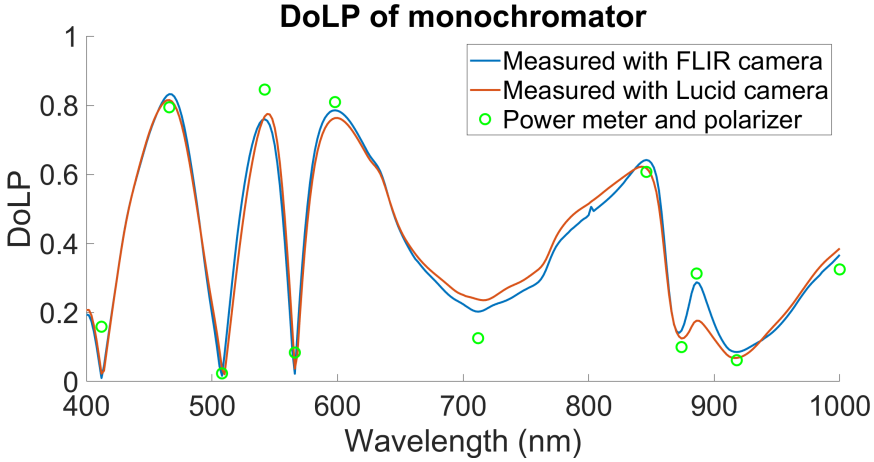

Figure 2. DoLP of the monochromator output as measured by the FLIR camera, the Lucid camera, and an optical power meter and polarizer.

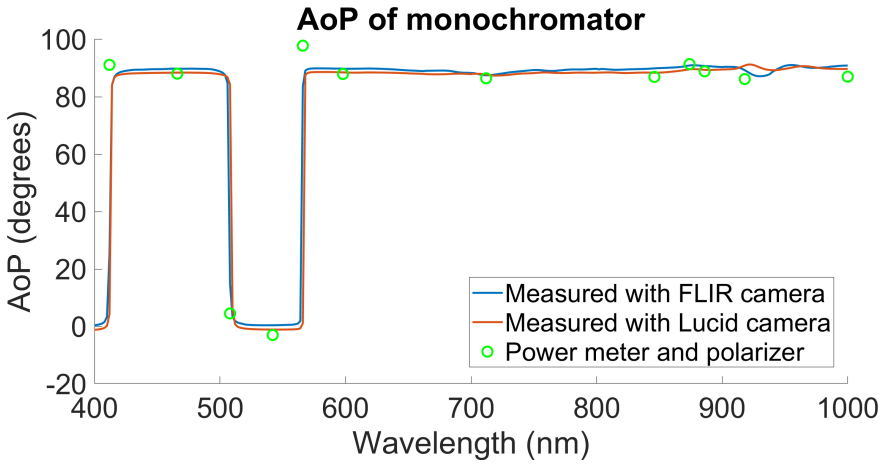

Figure 3. AoP of the monochromator output as measured by the FLIR camera, the Lucid camera, and an optical power meter and polarizer.

polarized output. However, the detector can measure the linear Stokes vector at each super pixel. Therefore, we assumed the individual subpixels in a super pixel had uniform response and used Eq. 1 to calculate S_0 at each super pixel and determine the RSR for a super pixel.

It should be noted that instead of removing the camera polarization sensitivity by using a sum of polarization components, it is also possible to remove the polarization of the monochromator. This could be done, for example, by putting the monochromator output into an integrating sphere, though this quickly leads to photon-starved measurements. Alternatively, it may be possible to compute a value of S_0 at each subpixel by rotating the camera and taking measurements with the camera oriented horizontally and vertically. However, the spatial non-uniformity of the monochromator output might make this challenging, as individual super pixels would be imaging different parts of the monochromator output as the camera is rotated.

To measure an RSR curve for each camera, the power output by the monochromator at each wavelength was first measured using an optical power meter. Next, the DoFP camera detector was positioned to measure the monochromator output, and an image was recorded at each wavelength as the monochromator grating was scanned. At each super pixel, S_0 was calculated, and the S_0 values were averaged over all the super pixels in the region of interest. Finally, the average S_0 at each wavelength was divided by the corresponding optical power, and the curve was normalized to its maximum. The RSRs found for each camera are shown in Fig. 4.

As an example of what happens when a partially polarized monochromator output is used to measure the RSR of a polarization-sensitive detector, the data were reprocessed in an incorrect way, analyzing individual (polarized) subpixels instead of using S_0 at each super pixel. An incorrect I_{0° RSR was found by averaging all of the I_{0° subpixels in the region of interest. This was done for all four subpixels, and the results for one camera are shown in Fig. 5.

5. DISCUSSION AND CONCLUSIONS

The measurements of the monochromator output revealed that its polarization is strong and varies significantly as a function of wavelength. Therefore, the polarization is changing as the angle of the diffraction grating in the monochromator is changed. Specifically, the DoLP of the monochromator swings from minima lower than 0.1 to maxima higher than 0.7, and the AoP is vertical over most of the spectral range but horizontal from 508 to 564 nm. While reflections from mirrors in the monochromator can contribute to the observed polarization, the polarizing effect of the mirrors is expected to be smaller and spectrally flatter than what was observed. Thus, the diffraction grating was determined to be the likely dominant source of spectral variation in the output polarization.

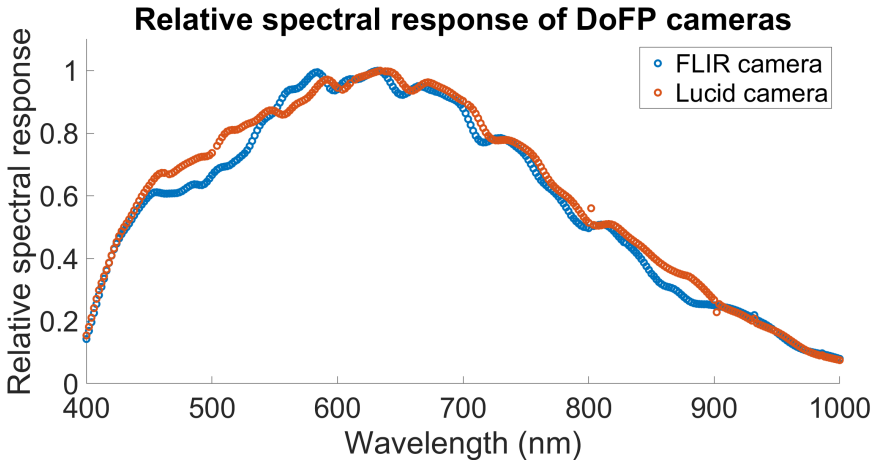

Figure 4. Relative spectral response curve determined from the sum of polarized subpixel outputs for the DoFP cameras. One outlier was removed from the FLIR data, and six outliers were removed from the Lucid data.

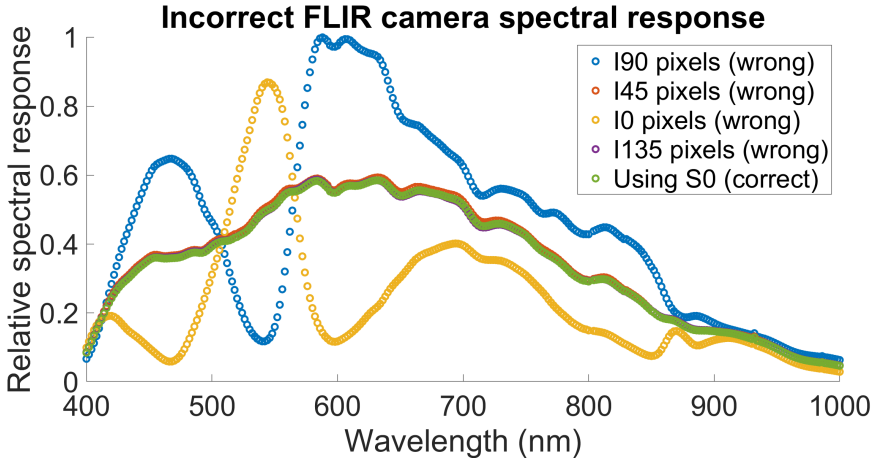

Figure 5. Incorrect relative spectral response curve determined from analyzing each polarized subpixel without accounting for the monochromator output polarization, plotted over correct RSR.

The polarization of the monochromator output makes it difficult to perform a spectral characterization of a pixelated polarized imager. A method of analysis to characterize the RSR of a DoFP camera with direct illumination from a monochromator was shown. The incorrect results that occur from analyzing the data as if the monochromator output were randomly polarized showed that errors exceeding 100% occurred when the source polarization was ignored for measuring the RSR of a polarization-sensitive camera. Therefore, just as the intentional or unintentional polarization sensitivity of an instrument must be characterized when making measurements of polarized light, it is necessary to characterize the polarization of a source before using that source to measure the spectral response of a polarization-sensitive instrument.

This study assumed that the subpixels in each super pixel had a uniform response, and it largely avoided consideration of spatial non-uniformity in the monochromator output by averaging the RSRs of all super pixels in a region of interest. Future work will explore the use of a radiometric calibration to account for differences in the response of individual subpixels. We also will look at differences in the RSRs of different super pixels to study the spatial non-uniformity of the monochromator output. Finally, additional studies are being done in our group to characterize the polarization sensitivity of hyperspectral imagers. Those polarization sensitivity responses may also be caused by a diffraction grating in the imager, and we plan to compare the results from both of these studies.

ACKNOWLEDGMENTS

This material is based upon work supported in part by the National Science Foundation EPSCoR Cooperative Agreement OIA-1757351 and in part by the U.S. Air Force Research Laboratory with a subcontract through S2 Corp.

REFERENCES

[1] Corrons, A. and Zalewski, E. F., "Detector Spectral Response From 350 to 1200 nm Using a Monochromator Based Spectral Comparator," Technical Note 988, National Bureau of Standards (1978).

[2] Boivin, L.-P., "Study of bandwidth effects in monochromator-based spectral responsivity measurements," *Appl. Opt.* **41**(10), 1929–1935 (2002).

[3] Barsi, J. A., Lee, K., Kvaran, G., Markham, B. L., , and Pedelty, J. A., "The Spectral Response of the Landsat-8 Operational Land Imager," *Remote Sens.* **2014**(6), 10232–10251 (2014).

[4] Bücher, K. and Schönecker, A., "Spectral Response Measurements of Multi-Junction Solar Cells with a Grating Monochromator and a Fourier Spectrometer," *Tenth E.C. Photovoltaic Solar Energy Conference*, 107–110 (2017).

[5] Hashimoto, T., Dahl, L. M., Laurie, S. A., and Shaw, J. A., "Camera characterization for all-sky polarization measurements during the 2017 solar eclipse," *Proc. SPIE* **10407**, 1040706 (2017).

[6] Gravrand, O., Wlassow, J., and Bonnefond, L., "A calibration method for the measurement of IR detector spectral responses using a FTIR spectrometer equipped with a DTGS reference cell," *Proc. SPIE* **9154**, 91542O (2014).

[7] Brown, S. W., Eppeldauer, G. P., and Lykke, K. R., "Facility for spectral irradiance and radiance responsivity calibrations using uniform sources," *Appl. Opt.* **45**(32), 8218–8237 (2006).

[8] Schuster, M., Nevas, S., Sperling, A., and Völker, S., "Spectral calibration of radiometric detectors using tunable laser sources," *Appl. Opt.* **51**(12), 1950–1961 (2012).

[9] Mahmoud, K., Park, S., and ad Dong-Hoon Lee, S.-N. P., "Measurement of normalized spectral responsivity of digital imaging devices by using a LED-based tunable uniform source," *Appl. Opt.* **52**(16), 1263–1271 (2013).

[10] Furxhi, O., Haefner, D., and Burks, S., "Instrument for the measurement of normalized spectral response of cameras in the thermal bands," *Proc. SPIE* **10625**, 0162503 (2018).

[11] Toivonen, M. E. and Klami, A., "Practical Camera Sensor Spectral Response and Uncertainty Estimation," *J. Imaging* **2020**(6), 79 (2020).

[12] Tyo, J. S., Goldstein, D. L., Chenault, D. B., and Shaw, J. A., "Review of passive imaging polarimetry for remote sensing applications," *Appl. Opt.* **45**(22), 5453–5469 (2006).

[13] Pust, N. J. and Shaw, J. A., "Dual-field imaging polarimeter using liquid crystal variable retarders," *Appl. Opt.* **45**(22), 5470–5478 (2006).

[14] Young, J., Knight, E., and Merrow, C., "MODIS polarization performance and anomalous four-cycle polarization phenomenon," *Proc. SPIE* **3439**, 246–256 (1998).

[15] Shaw, J. A., "The Effect of Instrument Polarization Sensitivity on Sea Surface Remote Sensing with Infrared Spectroradiometers," *J. Atmos. Oceanic Technol.* **19**, 820–827 (2002).

[16] Sun, J.-Q. and Xiong, X., "MODIS Polarization-Sensitivity Analysis," *IEEE Transcations on Geoscience and Remote Sensing* **45**(9), 2875–2885 (2007).

[17] Taylor, J. K., Revercomb, H. E., and Tobin, D. C., "An Analysis and Correction of Polarization Induced Calibration Errors for the Cross-track Infrared Sounder (CrIS) Sensor," *Light, Energy and the Environment 2018 (E2, FTS, HISE, SOLAR, SSL)*, FW2B.3, Optical Society of America (2018).

[18] Angal, A., Geng, X., Xiaoxiong, Twedt, K. A., Wu, A., Link, D. O., and Aldoretta, E., "On-Orbit Calibration of Terra MODIS VIS Bands Using Polarization-Corrected Desert Observations," *IEEE Transcations on Geoscience and Remote Sensing* **58**(8), 5428–5439 (2020).

[19] Maruyama, Y., Terada, T., Yamazaki, T., Uesaka, Y., Nakamura, M., Matoba, Y., Komori, K., Ohba, Y., Arakawa, S., Hirasaw, Y., Kondo, Y., Murayama, J., Akiyama, K., Oike, Y., Sato, S., and Ezaki, T., "3.2-MP Back-Illuminated Polarizationi Image Sensor With Four-Directional Air-Gap Wire Grid and 2.5-μm Pixels," *IEEE Transcations on Electron Devices* **65**(6), 2544–2551 (2018).

[20] Sandus, O., "A Review of Emission Polarization," *Appl. Opt.* **4**(12), 1634–1642 (1965).
[21] Spooner, D., "Polarization Pattern of a High Intensity Incandescent Lamp," *Appl. Opt.* **11**(12), 2984–2986 (1972).
[22] Kostuk, R. K., "Polarization characteristics of a 100-W FEL-type filament lamp," *Appl. Opt.* **20**(13), 2181–2182 (1981).
[23] Voss, K. J. and da Costa, L. B., "Polarization properties of FEL lamps as applied to radiometric calibration," *Appl. Opt.* **55**(31), 8829–8832 (2016).